

# Store Separation from Cavities at Supersonic Flight Speeds

Robert L. Stallings Jr.\*

NASA Langley Research Center, Hampton, Virginia

An experimental investigation has been conducted to determine the aerodynamic characteristics of a typical wing-control missile configuration during separation from a box-type cavity having depth-to-length ratios ( $D/L$ ) ranging from 0.088 to 0.225. The cavity was located in a splitter plate that spanned the low Mach number test section of the Langley Unitary Plan Wind Tunnel. Aerodynamic characteristics are presented for Mach 2.36 and a freestream unit Reynolds number of  $6.6 \times 10^6/\text{m}$ . For the shallow cavity ( $D/L = 0.088$ ), large interactions existed between the cavity and the flat plate flowfield which resulted in unfavorable separation characteristics for the missile model. For the deep cavity ( $D/L = 0.225$ ), the flat plate flowfield essentially bridged the cavity resulting in minor interactions and favorable separation characteristics for the missile model.

## Nomenclature

$A$	= model reference area, $\pi d^2/4$
$C_m$	= pitching-moment coefficient, pitching moment/ $q_\infty A l$
$C_N$	= normal-force coefficient, normal force/ $q_\infty A$
$C_p$	= pressure coefficient, $(p - p_\infty)/q_\infty$
$d$	= store-model diameter
$D$	= cavity depth
$l$	= store-model length
$L$	= cavity length
$M$	= freestream Mach number
$p$	= local measured static pressure
$p_\infty$	= freestream static pressure
$q_\infty$	= freestream dynamic pressure
$s$	= wing span
$S_c$	= surface length on cavity ceiling relative to cavity front face (see Fig. 5)
$S_{FF}$	= surface length on cavity front-face relative to flat plate surface (see Fig. 5)
$S_{RF}$	= surface length on cavity rear-face relative to cavity ceiling (see Fig. 5)
$t$	= time relative to store ejection
$W$	= cavity width
$x, y$	= store-model coordinates relative to nose tip
$Z$	= perpendicular distance from splitter plate surface
$\alpha$	= angle of attack relative to flat plate surface

## Introduction

**B**OTH internal and conformal carriage of stores are being considered for future supersonic military aircraft in order to minimize aerodynamic drag, aerodynamic heating, and radar signature. In order to realize full advantage of the aircraft supersonic flight speeds, it is desirable to have the capability of releasing the stores at supersonic speeds. Although there is considerable information available in the literature concerning acoustic measurements in cavities and bomb bays, there is very little information available concerning the aerodynamic characteristics of stores during separation from conformal and internal carriage configurations at supersonic speeds. Therefore, an exploratory wind-tunnel test was initiated to determine the near-field separation characteristics of a typical wing-control missile configuration from a box cavity of various depths. The box cavity was located in a splitter plate that spanned the low

Mach number test section of the Langley Unitary Plan Wind Tunnel. Tests were conducted at Mach numbers from 2.36 to 2.86 for cavity depth-to-length ratios ranging from 0.088 to 0.225.

Results presented and discussed are cavity pressure distributions, cavity oil flows, and store aerodynamic characteristics in the cavity flowfield.

## Test Facility, Models, and Instrumentation

The tests were conducted in the low-speed leg of the Langley Unitary Plan Wind Tunnel, which is a variable-pressure, continuous-flow facility described in detail in Ref. 1. An asymmetric sliding block nozzle leads to the test section and permits a continuous variation in Mach number from about 1.50 to 2.86. The present tests were conducted at Mach numbers of 2.36 and 2.86 at a constant Reynolds number of  $6.6 \times 10^6/\text{m}$ .

The parent aircraft for the present test was represented by a vertical splitter plate that extended from the floor to the ceiling of the test section as shown in Fig. 1. The splitter plate was 121.9 cm high and 182.9 cm in length. The leading edge of the cavity was located 72.4 cm downstream of the plate leading edge. The plate boundary layer was artificially tripped using a band of No. 50 grit located 1.5 cm downstream from the leading edge. The splitter plate was selected as the parent body for several reasons. First, it was desired to have a well-defined basic flowfield approaching the cavity in order to be able to clearly define the effects of the cavity flowfield on the store separation characteristics, and second, the plate was readily available and could be used for the present tests with only minor modifications. In addition, the length of the boundary layer run ahead of the cavity (72.4 cm) when scaled to full-scale conditions based on the scale of the store models tested is representative, in many cases, of the boundary layer run ahead of store locations for existing aircraft. Once the effects of the basic box-cavity flowfield are established, subsequent tests are planned to determine how changes of the parent body configuration perturb the cavity flowfield and the resulting store separation characteristics.

Shown in Fig. 2 is a photograph of a Sparrow missile model attached to the offset sting assembly that was used to position the models relative to the cavity. The offset sting allowed the models to be positioned inside the cavity. The sting assembly was attached to the test section model support assembly, which could be remotely varied in either the lateral or longitudinal direction.

Results presented in this paper were actually obtained from two tests using two different store models and two different box-cavity configurations. The test programs are identified as the "Sparrow model" tests and the "generic wing-control

Presented as Paper 82-0372 at the AIAA 20th Aerospace Sciences Meeting, Orlando, Fla., Jan. 11-14, 1982; submitted Feb. 5, 1982; revision received Sept. 23, 1982. This paper is declared a work of the U.S. Government and therefore is in the public domain.

\*Aerospace Engineer, Supersonic Aerodynamics Branch, High-Speed Aerodynamics Division, Associate Fellow AIAA.

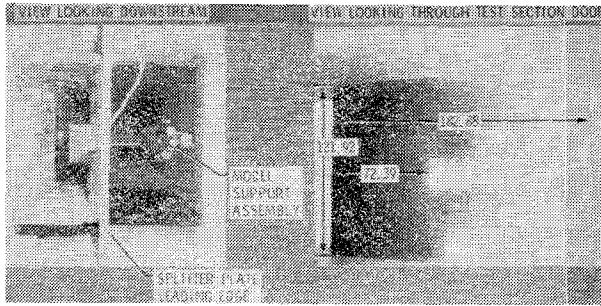


Fig. 1 Photographs of a flat plate assembly installed in a low Mach number test section.

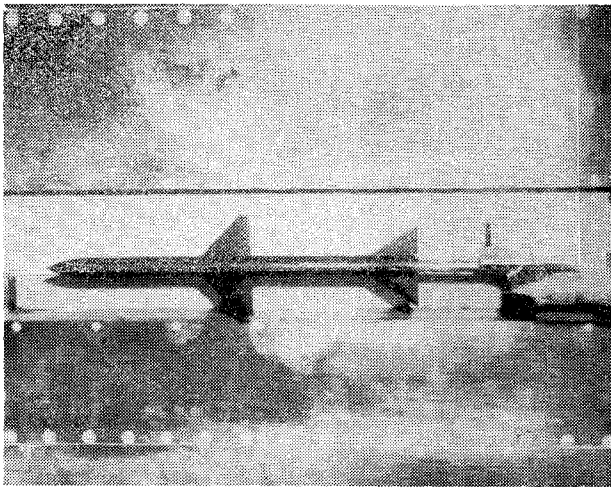


Fig. 2 Typical store model installation.



Fig. 3 Photograph of store models.

model" tests. The stores used in the two tests were basically the same as shown in Fig. 3 and the tabulated model information given in Fig. 4. The Sparrow model was an existing Sparrow III-type missile model that was previously tested in the Unitary tunnel with results presented in Ref. 2. The generic wing-control model is basically a stretched version of the Sparrow model and, as shown in Fig. 4, had a  $l/d$  ratio of 20.0 as compared to 18.0 for the Sparrow model. The generic wing-control model is one of a group of generic models that are being constructed for additional carriage and separation studies. Both models had a body diameter of 3.0 cm and a wing span of 15.2 cm. The wings and tails have the same relative locations on the body for the two models as shown by the store geometry insert of Fig. 4. Basic cavity dimensions for the two test programs are also shown in Fig. 4. For the Sparrow model test, store forces and moments and cavity oil flows were obtained for a cavity having a  $D/L$  ratio of 0.088 and a  $W/L$  ratio of 0.214. For the generic wing-control model tests, store forces and moments were obtained for a much

TEST	STORE DIMENSIONS			CAVITY DIMENSIONS			DATA
	$l/d$	$s/d$	$l$ , cm	$D/L$	$W/L$	$L$ , cm	
SPARROW MODEL	18.0	5.0	54.9	.088	.214	94.9	STORE FORCES AND MOMENTS, CAVITY OIL FLOW
GENERIC WING-CONTROL MODEL	20.0	5.0	61.0	.052 TO .225	.225	84.8	CAVITY PRESSURES
	20.0	5.0	61.0	.225	.225	84.8	STORE FORCES AND MOMENTS

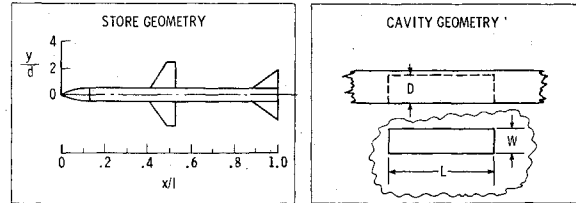


Fig. 4 Model geometry and dimensions.

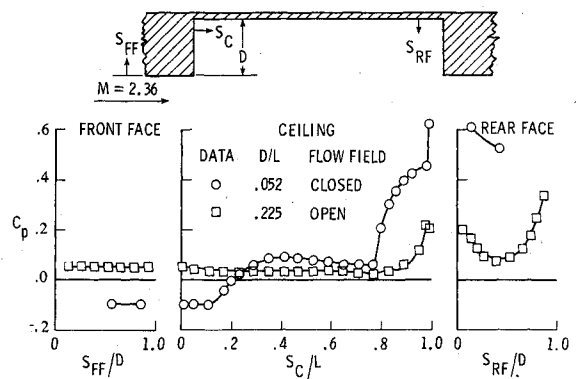


Fig. 5 Effect of cavity depth on cavity pressure distributions.

deeper cavity ( $D/L$  ratio of 0.225) having about the same value of  $W/L$  as the Sparrow tests. Cavity pressure measurements were also obtained for the generic model tests for cavity  $D/L$  ratios ranging from 0.052 to 0.225. The cavity pressure orifices were located along the longitudinal centerline of the cavity front face, ceiling, and rear face.

The pressures were measured by electrical transducers connected to a pressure scanning system. A total of three scanners were used with tubing from approximately 20 orifices connected to each scanner. Three reference pressures were also connected to each scanner to provide transducer calibrations for each data point. Force and moment measurements were obtained using a six-component strain-gage balance; however, in the present paper only normal force and pitching moment coefficients are presented.

### Results and Discussion

Shown in Fig. 5 is the effect of cavity depth on cavity centerline pressure distributions. Results are presented for the front face, ceiling, and rear face of the cavities having depth-to-length ratios of 0.052 and 0.225. Increased cavity depth has a very large effect on the cavity pressure distribution. Such an effect has been observed by other investigators,<sup>3-5</sup> and is associated with the shear layer that originates at the cavity front face attaching to the cavity ceiling for the case of the shallow cavity and bridging the cavity for the case of the deep cavity. For the shallow cavity, the flow separates at the front face and reattaches downstream on the cavity ceiling in the vicinity of  $S_c/L=0.3$ . The flow expansion at the front face results in the reduced pressures for  $0 \leq S_c/L < 0.3$ . Another distinct and independent separation of the flow occurs further downstream ahead of the rear face which appears as a forward facing step to the oncoming cavity flow. The pressure distribution measured between  $0.75 < S_c/L \leq 1.0$  is characteristic of the flow ahead of a forward facing step. The large adverse pressure gradient in this region results from the flow

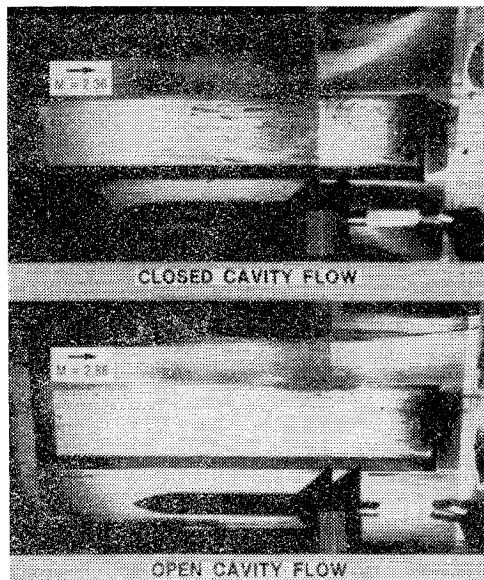


Fig. 6 Oil flow photographs of open and closed cavity flows;  $D/L = 0.088$ : a) closed cavity flow; b) open cavity flow.

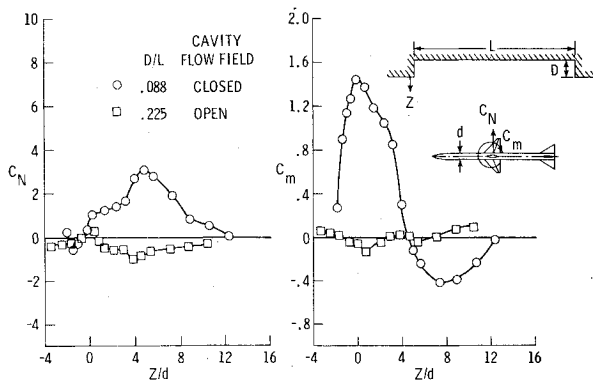


Fig. 7 Effect of cavity depth on store model separation characteristics,  $M = 2.36$ .

separating ahead of the step and turning through the large angle required to exit over the rear face. Large pressures for this case are also measured on the rear face. For the deep cavity, the shear layer bridges the cavity and impinges on the rear face near the plate surface. The very small turning angle of the shear layer at the front face results in essentially uniform pressures approximately equal to freestream static pressure on the front face and the ceiling for  $S_c/L < 0.8$ . The larger pressures measured on the ceiling for  $S_c/L > 0.8$  and on the rear face are associated with the shear layer impinging on the rear face. The cavity flowfields depicted by the pressure distributions shown in Fig. 5 are generally referred to in the literature as "closed" cavity flow for the case shown for  $D/L = 0.052$  and as "open" cavity flow for the case shown for  $D/L = 0.225$ .

Examples of closed and open cavity flows are further illustrated by the oil flow photographs shown in Fig. 6. These results were obtained during the Sparrow model tests and are presented for a cavity of fixed depth ( $D/L = 0.088$ ) at Mach numbers of 2.36 and 2.86. These results indicate that the type cavity flowfield also depends upon Mach number as well as depth-to-length ratio. In general, the closed and open flowfields characterized by the oil flow photographs shown in Figs. 6a and 6b, respectively, are consistent with the flowfields reasoned from the pressure distributions shown in Fig. 5.

The results presented in Figs. 5 and 6 show that for the case of closed cavity flows, large interactions occur between the

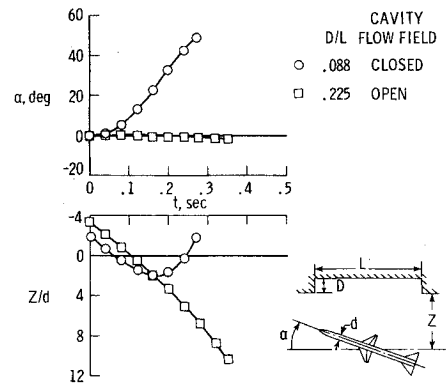


Fig. 8 Effect of cavity depth on trajectory of full-scale missile using simplified two-degree-of-freedom analysis and measured aerodynamic characteristics,  $M = 2.36$ ,  $q = 4.79$  kPa.

flowfield and the cavity, whereas for the case of open cavity flows relatively minor interactions occur. The large interactions of the closed cavity flow would be expected to have significant effects on store aerodynamic characteristics during separation and the determination of this effect is the primary purpose of this study. Shown in Fig. 7 are measured normal-force coefficients and pitching-moment coefficients for a wing-control store-model during separation through both a closed and an open cavity flowfield. Actually, the results shown are for two different store models: the Sparrow model and the generic wing-control model. However, due to the similarity of these two models, as shown in Fig. 4, the effects shown in Fig. 7 can be attributed primarily to flowfield differences rather than model geometry differences. In order to facilitate safe separation of the store from the cavity, the values of both  $C_N$  and  $C_m$  should be near zero or slightly negative. The data show that this trend exists for the open cavity flow; for the closed cavity flow, however, large positive values of both  $C_N$  and  $C_m$  are measured with the store in the cavity flowfield. The large positive pitching moments are a result of the model nose being located in an upwash field created by the flow expanding into the cavity and the model tail being located in a downwash created by the flow exiting from the cavity.

The aerodynamic characteristics shown in Fig. 7 were used to make simplified two-degree-of-freedom trajectory calculations (Eqs. 7 and 12 of Ref. 6) for a typical full-scale wing-control missile separating from a cavity into both an open and closed cavity flowfield with an ejection velocity of 6.1 m/s. These results are presented in Fig. 8. To obtain the results shown in Fig. 8, it was necessary to know values of  $C_N$  and  $C_m$  for  $\alpha \leq 0$  as well as for  $\alpha \geq 0$ . The values for  $\alpha \leq 0$  were not measured in the present tests, but were estimated from the equations:

$$(C_N)_\alpha = (C_N)_{\alpha=0} + (dC_N/d\alpha)\alpha$$

$$(C_m)_\alpha = (C_m)_{\alpha=0} + (dC_m/d\alpha)\alpha$$

where values of  $dC_N/d\alpha$  and  $dC_m/d\alpha$  were assumed to correspond to freestream values and were determined from the data of Ref. 2. Presented in Fig. 8 are the variations with time of missile angle of attack and separation distance relative to the plate surface. For the closed cavity flowfield, the large positive pitching-moment coefficients result in the missile angle of attack increasing very rapidly after ejection. The resulting increase in lift combined with the lift at  $\alpha = 0$  shown in Fig. 7 results in the missile being forced back into the cavity, even though it had an initial downward ejection velocity of 6.1 m/s and a mass of approximately 227 kg. For the case of the open cavity flowfield, the missile angle of attack remains approximately zero and falls through the cavity flowfield without incident.

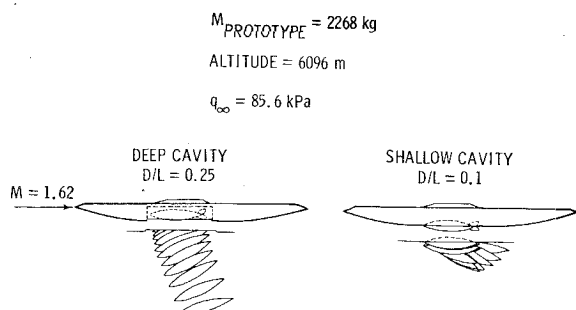


Fig. 9 Results from wind-tunnel bomb release tests at supersonic speeds.

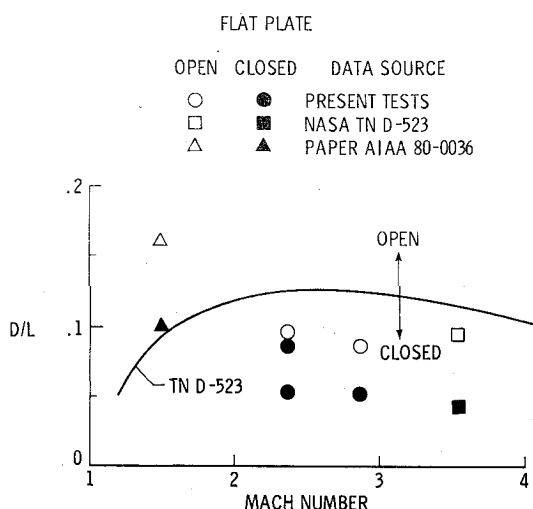


Fig. 10 Comparison of measured and predicted critical depth-to-length ratios for cavities in a flat plate.

Although very limited information is available in the literature concerning store separation characteristics for a closed cavity flowfield, one source<sup>7</sup> was found that reports results from bomb release tests for a variety of cavity configurations at supersonic speeds, some of which apparently had closed cavity flow. The parent body for these tests was a fuselage that consisted of a circular cylinder streamlined fore and aft with part of the upper half removed. The cavities, or bomb bays, were located at approximately midlength of the fuselage. The bomb model for these tests simulated a 2268 kg bomb and the trajectories for the drop tests were determined using high-speed motion picture photography. Shown in Fig. 9 are drop-test trajectories from two cavities having values of  $D/L$  that are about the same as for the results shown in Fig. 8. It should be noted that although the deep cavity shown in Fig. 9 is a box-type cavity, the shallow cavity is more of a contoured cavity matching the bomb contour and has a maximum  $D/L$  ratio of 0.1. The bomb trajectories show that for the deep cavity, the bomb separates cleanly, whereas for the shallow cavity, it pitches up shortly after release and regresses back into the fuselage. This effect of cavity depth on store separation characteristics is consistent with the present wind-tunnel results presented in Fig. 7.

Results presented herein show that stores separating from cavities in a flat plate having open and closed flowfields have radically different separation characteristics and that the type of flowfield is dependent upon cavity depth-to-length ratio and freestream Mach number. Shown in Fig. 10 is an empirical curve from Ref. 5 showing the variation with Mach number of the critical depth-to-length ratio between open and closed cavity flows. This curve is based on experimental data

obtained behind aft facing steps and ahead of forward steps. Values of  $D/L$  greater than the critical values correspond to open cavity flows, whereas values less than the critical values correspond to closed cavity flows. Also presented in Fig. 10 are measured data from the present tests and from the literature where the type cavity was determined from either pressure tests or oil flow tests. The solid symbols represent experimentally determined closed cavity flows and should fall below the critical curve, whereas the open symbols represent open cavity flows and should fall above the critical curve. The experimental data indicate that the critical curve should occur at lower values of  $D/L$  than predicted for  $M > 2$ . The data also suggest a continuous decrease in the critical  $D/L$  values with increasing Mach number, whereas the prediction indicates the critical values of  $D/L$  increase with increasing Mach number for  $M < 2.5$  and decrease with Mach number for greater Mach numbers.

Additional tests are planned using some of the existing hardware to provide a more complete data base describing the box-cavity flowfield and associated store separation characteristics. These tests will be conducted for a large number of cavity depth-to-length ratios for freestream Mach numbers from 1.5 to 3.0. Once the effects of the flat plate and box-cavity flowfield are defined, store separation characteristics will be measured in the cavity flowfield of more representative parent body configurations. Additional variables being considered for future tests consist of cavity geometry, store geometry, and store angle of attack.

### Concluding Remarks

An experimental investigation has been conducted to determine the aerodynamic characteristics of a typical wing-control missile configuration during separation from a box-type cavity having depth-to-length ratios ( $D/L$ ) ranging from 0.088 to 0.225. The cavity was located in a splitter plate that spanned the low Mach number test section of the Langley Unitary Plan Wind Tunnel. Aerodynamic characteristics are presented for Mach 2.36 and a freestream unit Reynolds number of  $6.6 \times 10^6/\text{m}$ . Results from these tests lead to the following concluding remarks:

1) For the shallow cavity ( $D/L = 0.088$ ), large interactions existed between the cavity and the flat plate flowfield which resulted in unfavorable separation characteristics for the missile model.

2) For the deep cavity ( $D/L = 0.225$ ), the flat plate flowfield essentially bridged the cavity, resulting in minor interactions and favorable separation characteristics for the missile model.

### References

- Jackson, C.M. Jr., Corlett, W.A., and Monta, W.J., "Description and Calibration of the Langley Unitary Plan Wind Tunnel," NASA TP 1905, Oct. 1981.
- Monta, W.J., "Supersonic Aerodynamic Characteristics of a Sparrow III Type Missile Model with Wing Controls and Comparison With Existing Tail-Control Results," NASA TP 1078, Nov. 1977.
- Charwat, A.F., Rous, J.N., Dewey, F.C., and Hitz, J.A., "An Investigation of Separated Flows," *Journal of Aerospace Sciences*, Vol. 28, Pt. I, June 1961, pp. 457-470, Pt. II, July 1961, pp. 513-527.
- Clark, R.L., Kaufman, L.G. II, and Maciulaitis, A., "Aeroacoustic Measurements for Mach 0.6 to 3.0 Flows Past Rectangular Cavities," AIAA Paper 80-0036, Jan. 1980.
- McDearmon, R.W., "Investigation of the Flow in a Rectangular Cavity in a Flat Plate at a Mach Number of 3.55," NASA TN D-523, 1960.
- Sandahl, C.A. and Faget, M.A., "Similitude Relations for Free-Model Wind-Tunnel Studies of Store-Dropping Problems," NACA TN 3907, Jan. 1957.
- Rainey, R.W., "A Wind-Tunnel Investigation of Bomb Release at a Mach Number of 1.62," NACA RM L53L29, March 1954.